Int. J. Solids Structures Vol. 30, No. 1, pp. 37–60, 1993
Printed in Great Britain.

0020–7683/93 $5.00+ .00

STABILITY ANALYSIS OF INHOMOGENEOUS, FIBROUS COMPOSITE PLATES

MAHESH D. PANDEY and ARCHIBALD N. SHERBOURNE
Solid Mechanics Division, Dept. of Civil Engineering, University of Waterloo, Waterloo, Ontario, Canada N2L 3G1

(*Received* 18 *January* 1991; *in revised form* 5 *June* 1991)

Abstract—Materials with deliberately designed forms of anisotropy and inhomogeneity, obtained by manipulating microstructural composition, can provide excellent solutions to existing design constraints and create new design opportunities. This new class of problems, concerning optimization of the internal structures of elastic bodies, is the subject matter of the present investigation. The paper focuses attention on deliberately designed inhomogeneity by controlling spatial fiber distribution in a lamina, for improving uniaxial and shear buckling behavior of rectangular, unidirectional and cross-ply laminates under a variety of boundary conditions. In the literature, optimization of the orientation of fibers (through thickness) in fibrous composite laminates with respect to the buckling load is discussed extensively on the assumption of uniform spatial fiber distribution in the plane of the plate. Design involving non-uniform fiber distribution, which has received much less attention, appears to be an attractive option, at least from a theoretical point of view. Also, the motivation comes from reinforced concrete structures where the non-uniform spacing of reinforcing bars is quite common practice.

Non-uniform fiber distribution leads to the problem of inhomogeneous, orthotropic plate buckling which is solved in two steps. Firstly, the prebuckling stress field is derived because the assumption of uniform, uniaxial stress, common in homogeneous plates, is theoretically no longer valid. Finally, out-of-plane buckling is analysed incorporating the prebuckling field derived earlier. Within the framework of the Ritz method, a stress function formulation for plane-stress (stretching) and a displacement formulation for buckling analysis, are employed. An important feature of the analysis is using the classical analogy between in-plane stress function and out-of-plane buckling displacement formulations which not only provides a unified analytical treatment but also reduces the problem size significantly. For the analysis, a computerized Rayleigh–Ritz method, in conjunction with Gram–Schmidt orthogonal polynomials as coordinate functions, is developed, which is capable of modeling a variety of boundary conditions, *viz.* simple, clamped, free and their combinations.

Uniaxial and shear buckling coefficients of unidirectional and cross-ply laminates are computed for various cases of sinusoidal fiber distribution. It is found that, for given constant fiber volume, a higher fiber concentration at the middle of the plate would generally increase the buckling load by as much as 25% over a uniform distribution of the same amount of fibers. The paper highlights the unusual tailoring capabilities offered by advanced composite materials.

NOTATION

a	length of plate along x-axis
b	width of plate along y-axis
B.C.	boundary condition
C_P	cross-ply ratio
D_f	$E_f t^3/12$
D_{ij}	bending stiffness matrix of a laminate
E_f, E_m	modulus of elasticity of fiber and matrix, respectively
F	Airy's stress function
N_P	total number of plies
N_v	ratio of V_f at the plate centre to the edge
N_x, N_{xy}	non-dimensional uniaxial and shear buckling coefficients
R_1	E_m/E_f
R_2	ν_m/ν_f
t	plate thickness
U.D.	unidirectional laminates
V_f	fiber volume fraction
W	non-dimensional plate deflection
X	non-dimensional length ($= x/a$)
Y	non-dimensional width ($= y/b$)
β	plate aspect ratio (a/b)
ν_f, ν_m	Poisson's ratio of fiber and matrix, respectively
σ_x, σ_y, σ_{xy}	in-plane stress resultants
σ_{x0}, σ_{xy0}	applied uniaxial and shear stresses, respectively.

INTRODUCTION

Among modern structural materials, the history of fiber-reinforced composites is barely three decades old. However, in this short period of time, there have been tremendous advances in the science and technology of this new class of materials. Low density, high strength, high stiffness to weight ratio, excellent durability and design flexibility of fiber-reinforced materials are the primary reasons for their use in many structural components in the aircraft, automotive, marine and other industries. The distribution and orientation of fibers, elastic properties of fibers and matrix and lamination sequence are the new degrees of freedom available to designers and their careful manipulation may significantly improve structural performance.

Optimization of the orientation of fibers (through thickness) in fibrous composite laminates with respect to the buckling load is discussed extensively in the literature (Hirano, 1979). In these exercises, the spatial distribution of fibers in the plane of the plate is assumed to be uniform. The present study focuses on finding the optimal spatial fiber distribution for fibrous composite plates under uniaxial compression (Fig. 1) and pure shear that would maximize its buckling load. The motivation has come from reinforced concrete structures where the non-uniform spacing of reinforcing bars is quite common practice. The study focuses attention on deliberately designed inhomogeneity, due to variable fiber distribution, for improving uniaxial and shear buckling behavior of rectangular laminates under a variety of boundary conditions (B.C.).

The concept of materials with deliberately designed forms of anisotropy and inhomogeneity obtained by manipulating microstructural composition can provide excellent solutions to existing design constraints and create new design opportunities. This new class of problems, concerning optimization of the internal structures of elastic bodies, is motivated from the composite nature of living tissues characterized by the presence of fibers, inclusions and voids in some three-dimensional patterns resulting in anisotropic, inhomogeneous and viscoelastic behavior. Oda (1988) emphasized the study of structural behavior of natural systems (plants and animals) for developing innovative design techniques and highlighted some of the distinctive features of the structural and material composition of bamboo. He reported that, in bamboo's cross-section, the radial distribution of fiber volume fraction is in accordance with the minimum weight design criterion. The fibers are distributed from the inner to outer surface in a non-linear fashion such that a higher concentration is found near the outer surface.

In an interesting study, Rammerstorfer (1974) reported that the optimal distribution of the Young's modulus of a simply-supported column was a parabolic function resulting in the highest possible increase in the buckling load of 21.6% over a uniform design. The optimality criterion proved to be that of constant curvature which led to a parabolic buckling mode contrary to the half sine wave (Euler mode) of a uniform column. Leissa and Vagins (1978) discussed the possibilities of designing a non-homogeneous material for a structural element of given dimensions and boundary and loading conditions such that the internal stress field is the desired optimum. Banichuk (1979) presented a comprehensive method for optimization of internal structure, basically fiber density and orientation, of anisotropic, inhomogeneous composites in a number of plane elasticity and plate bending

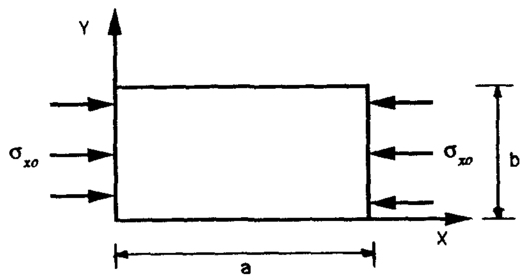

Fig. 1. Uniaxially loaded plate.

problems. An elaborate computational scheme was developed which was based on the minimum compliance optimality criterion. Banichuk and Kobelev (1981) considered the optimization of the internal structure of a simply-supported column made of randomly reinforced and macroscopically isotropic composite material. Using a Lagrange multiplier technique, the optimal distribution of the elastic modulus as a function of fiber volume fraction was found to be of sinusoidal nature, similar to that of Euler buckling. Kartvelishivli and Kobelev (1984) presented a rigorous mathematical formulation of optimization of fiber distribution in an inhomogeneous composite plate using variational calculus. Besides the mathematical complexity, which overshadowed the physics of the problem, results were obtained for limited cases of deflection, vibration and buckling of simply-supported plates. It was suggested that the optimal fiber distributions tend to follow the Rayleigh mode of vibration or buckling as the case may be. Bendsoe and Kikuchi (1988) suggested that shape optimization problems can be transformed to technologically more feasible material distribution problems using composite materials. They computed the optimal density of periodically distributed small holes (perforations) in a given homogeneous isotropic medium using the finite element method. The purpose was to minimize compliance for a given material and volume.

Our attention is drawn to a very recent research paper by Leissa and Martin (1990) on buckling and vibration analysis of inhomogeneous, unidirectional (0°) laminae using the Ritz method. The scope of this study was strictly limited to simply-supported plates while the present study offers a more general approach. Various additional analytical capabilities of our approach, compared to that of Leissa and Martin (1990), are discussed in greater length in the section entitled "Results and Discussions".

Most of the studies on material optimization, e.g. Banichuk, Kartvelishivli, etc., were based on formal optimization procedures such that the selection of design variables in a search for extremal solutions satisfying the prescribed criterion, was conducted in an objective fashion without depending on engineering intuition. Contrary to this, the literature on isotropic plates with optimal thickness distribution is based on more practical and physical observations. Spillers and Levy (1990) have shown mathematically that the optimal thickness distribution is proportional to the strain energy density in simply-supported isotropic plates. As the buckling mode for square plates involves half sine waves in both X and Y directions, this implies that a sinusoidal thickness distribution with higher values at the middle should provide an improved design. This hypothesis is contradicted by Parsons (1955) who showed a significant increase in the buckling load using a sinusoidal variation of thickness across the width (Y direction) of a simply-supported plate such that the thickness was higher at the edges than the middle. In an extreme case, with zero thickness at the centre and maximum at the edges ($Y = 0, 1$), the buckling load increases up to four times that of an equal volume, constant thickness plate. Similar observations were reported by Capey (1956) and Mansfield (1959) regarding step and linear variation of thickness, respectively, across the plate width. These observations have provided motivation for design of improved inhomogeneous composites, discussed herein, avoiding the formal optimization procedure.

Non-uniform fiber distribution leads to the problem of inhomogeneous, orthotropic plate buckling which is solved in two steps. Firstly, the derivation of the prebuckling stress field is required since the assumption of uniform, uniaxial stress, common in homogeneous plates, is no longer valid, at least from a theoretical point of view. The second step would be out-of-plane buckling analysis incorporating the prebuckling field derived earlier. Within the framework of the Ritz method, a stress function formulation for plane-stress (stretching) and displacement formulation for bucking analysis, are employed. An important feature of the analysis is using the classical analogy between in-plane stress function and out-of-plane buckling displacement formulations (Southwell, 1950) which not only provides a unified analytical treatment but also reduces the problem size significantly. For the analysis, a computerized Rayleigh–Ritz method, in conjunction with Gram–Schmidt orthogonal polynomials (Bhat, 1985) as coordinate functions, is developed, which is capable of modeling a variety of boundary conditions, *viz.* simple, clamped, free and their combinations.

ANALOGY BETWEEN STRETCHING AND BENDING PROBLEMS

The displacement, W, of a flat plate due to transverse loading, q, and the extensional Airy's stress function, F, in plane stress, is governed by differential equations (biharmonic) of identical form. This observation has served as the foundation for a well-developed mathematical analogue (or duality) between two physically independent problems of out-of-plane flexure and in-plane stretching in the field of variational calculus (Southwell, 1950; Elias, 1966). This duality between stretching and bending of plates allows for transforming the basic equations of one problem into the other by simply interchanging, according to certain correspondence, the dependent variables of the two problems. In the following section, the dual correspondence between stretching problem variables, *viz*. stress function, in-plane stresses, strains and change of curvature, and bending problem variables, *viz*. displacement, curvature, moment and transverse shears, respectively, are described. The discussion is intentionally limited to isotropic plates for the sake of simplicity and its generalization to orthotropic plates poses no theoretical problem.

Bending

The equilibrium of moments in the isotropic plate bending problem is given by

$$\frac{\partial^2 M_x}{\partial x^2}+2\frac{\partial^2 M_{xy}}{\partial x\,\partial y}+\frac{\partial^2 M_y}{\partial y^2}=q. \tag{1}$$

Recalling the moment-curvature

$$M_x = D(k_x+\nu k_y),\quad M_y = D(k_y+\nu k_x)\quad\text{and}\quad M_{xy} = D(1-\nu)k_{xy} \tag{2}$$

and curvature–displacement relationships

$$k_x = W_{,xx},\quad k_y = W_{,yy}\quad\text{and}\quad k_{xy} = W_{,xy}, \tag{3}$$

the equilibrium equation, (1), can be written as

$$W_{,xxxx}+2W_{,xxyy}+W_{,yyyy}=\frac{q}{D}, \tag{4}$$

where $D = Et^3/12(1-\nu^2)$ is the plate bending stiffness. Here, the subscripts preceded by a comma denote partial differentiation with respect to the corresponding coordinates. For example, $W_{,xx} = \partial^2 W/\partial X^2$.

Stretching

In-plane stresses, expressed in terms of Airy's stress function, F, by

$$\sigma_x = F_{,yy},\quad \sigma_y = F_{,xx}\quad\text{and}\quad \sigma_{xy} = -F_{,xy} \tag{5}$$

satisfy the following equations of equilibrium

$$\frac{\partial\sigma_x}{\partial x}+\frac{\partial\sigma_{xy}}{\partial y}=0\quad\text{and}\quad\frac{\partial\sigma_{xy}}{\partial x}+\frac{\partial\sigma_y}{\partial y}=0. \tag{6}$$

The condition for compatibility of the accompanying strains is

$$\frac{\partial^2\varepsilon_x}{\partial y^2}-\frac{\partial^2\gamma_{xy}}{\partial x\,\partial y}+\frac{\partial^2\varepsilon_y}{\partial x^2}=0 \tag{7}$$

which can be written in terms of a stress-function as (Haichang, 1984):

$$F_{,xxxx}+2F_{,xxyy}+F_{,yyyy}=0. \tag{8}$$

Analogy

A careful study of eqns (1)–(8) suggests the following analogy between variables of stretching and bending. Scalar quantities in the two problems are equivalent, e.g. stress function, F and displacement, W. Vector (tensor) quantities in the bending problem are at a phase difference of 90° from corresponding vector (tensor) quantities in the plane stress problem. Compatibility of curvatures and in-plane stress equilibrium are analogous

$$\begin{bmatrix} \sigma_x & \sigma_{xy} \\ \sigma_{xy} & \sigma_y \end{bmatrix} \cong \begin{bmatrix} k_y & -k_{xy} \\ -k_{xy} & k_x \end{bmatrix}. \tag{9}$$

Equations of moment equilibrium and in-plane strain compatibility are of similar form such that

$$\begin{bmatrix} \varepsilon_x & \dfrac{\gamma_{xy}}{2} \\ \dfrac{\gamma_{xy}}{2} & \varepsilon_y \end{bmatrix} \cong \begin{bmatrix} M_y & -M_{xy} \\ -M_{xy} & M_x \end{bmatrix}. \tag{10}$$

A detailed discussion can be found elsewhere (Elias, 1966).

Duality between boundary conditions

As seen in the previous section, variables of the bending and stretching problems are related to each other and, therefore, analogy between the boundary conditions of the two problems can be easily developed (Bassily and Dickinson, 1977). In general, force B.C.s in flexure correspond to geometrical B.C.s of stretching. A similar analogy has been employed in the conjugate beam method of calculating deflections of beams.

Simple supports in bending. Simply-supported conditions in bending specified as

$$W=0 \quad \text{and} \quad M_x=0 \quad (x=0) \tag{11}$$

would, from eqn (10), correspond to laterally restrained edges in stretching as given by

$$F=0 \quad \text{and} \quad \varepsilon_y=0 \quad (x=0). \tag{12}$$

Clamped supports in bending. A clamped edge is defined as

$$W=0 \quad \text{and} \quad W_{,x}=0 \quad (x=0); \tag{13}$$

the corresponding B.C.s in stretching would be

$$F=0 \quad \text{and} \quad F_{,x}=0 \quad (x=0). \tag{14}$$

Bending slope, a geomerical B.C., has no analogue in the stretching problem which implies free edge (no constraint) conditions in the stretching problem. Thus, a clamped B.C. in bending corresponds to free in-plane B.C.s. This fact is further elaborated by a specific example in the following section.

Free supports. At the free edges, bending moments and transverse shear forces are zero

Table 1. Duality between in-plane and out-of-plane boundary conditions

Out-of-plane	In-plane
Clamp (C)	Free (F)
Simple (S)	Simple (S)
Free (F)	Clamp (C)

$$M_x = M_y = Q_x = Q_y = 0 \quad (x = 0) \tag{15}$$

which means that strains and in-plane curvatures in stretching are zero:

$$\varepsilon_y = \varepsilon_x = \omega_y = -\omega_x = 0 \quad (x = 0). \tag{16}$$

Thus, out-of-plane free edges correspond to in-plane clamped edges.

Bassily and Dickinson (1977) have shown that a normally restrained in-plane edge corresponds to out-of-plane sliding edges. This duality between boundary conditions has been summarized in Table 1.

ANALYSIS

Fiber distribution

Inhomogeneous laminate designs are constructed using the following sinusoidal fiber distribution function

$$V_f(Y) = (V_f)_{avg}\left[\frac{1+(N_v-1)\sin\pi Y}{1+\frac{2}{\pi}(N_v-1)}\right]. \tag{17}$$

A similar function was employed by Parsons (1955) for describing various thickness distributions. Presently, N_v is the ratio of fiber volume fraction at the plate centre ($Y = 0.5$) to the edge ($Y = 0$) that defines the degree of non-uniformity and, also, the convex or concave nature of fiber distribution depending upon $N_v > 1$ or $N_v < 1$, respectively. $N_v \leqslant 1$ implies higher fiber concentration at the edges than the centre and the reverse is true when $N_v \geqslant 1$. $N_v = 1$ corresponds to uniform distribution with a fiber volume fraction of $(V_f)_{avg}$. This function, depending upon the value of N_v, simulates a variety of distributions as shown in Fig. 2. It should be emphasized that the total amount of fiber is constant and equal to that of a plate with uniform distribution and fiber volume fraction, $(V_f)_{avg}$. This function is very convenient to study the advantages of a non-uniform over uniform distribution for a given amount of fibers.

Martin and Leissa (1989) considered a parabolic variation of V_f from 0 at the edges to 1 at the centre which is reproduced herein as

$$V_f(Y) = 4Y(1-Y) \tag{18}$$

for the sake of comparison.

Constitutive relation

The constitutive relations for fibrous composite (Jones, 1975) can be restructured in terms of fiber modulus, E_f, as

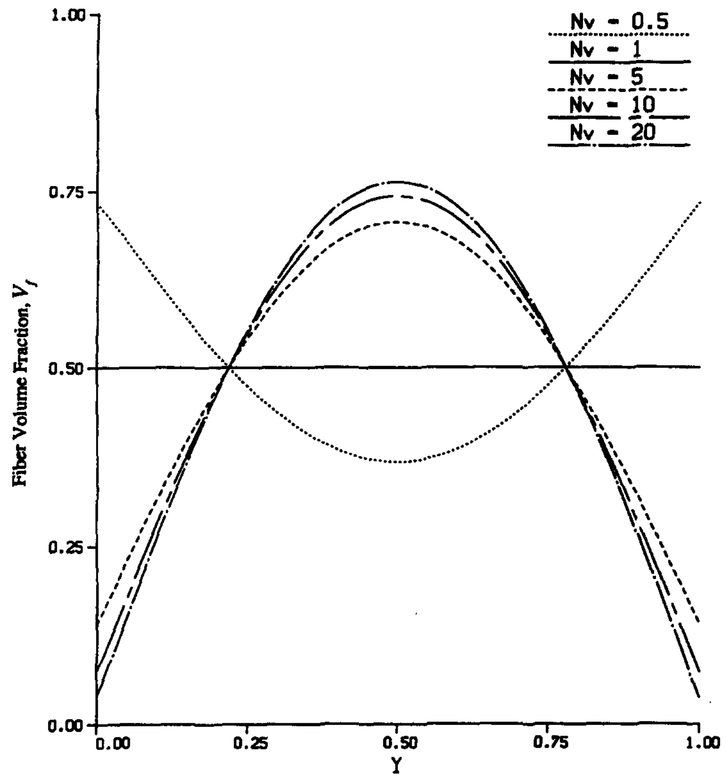

Fig. 2. Sinusoidal fiber distribution.

$$E_x = E_f[V_f + R_1(1-V_f)], \quad E_y = E_f\left[V_f + \frac{(1-V_f)}{R_1}\right]^{-1},$$

$$\nu_{xy} = \nu_f[V_f + R_2(1-V_f)], \quad G_{xy} = G_f\left[V_f + \frac{(1-V_f)}{R_3}\right]^{-1}, \tag{19}$$

where

$$G_f = \frac{E_f}{2(1+\nu_f)}, \quad R_1 = \frac{E_m}{E_f}, \quad R_2 = \frac{\nu_m}{\nu_f}, \quad R_3 = \frac{R_1(1+\nu_f)}{(1+R_2\nu_f)},$$

ν_m and ν_f are Poisson's ratio for fiber and matrix, respectively, and E_m is the matrix modulus of elasticity. All computations, in this paper, are carried out for T300 Graphite–Epoxy composite materials (Mallick, 1988) with the following elastic constants: $E_f = 220$ GPa, $E_m = 3.6$ GPa, $\nu_f = 0.20$ and $\nu_m = 0.35$ such that $R_1 = 0.01636$ and $R_2 = 1.75$. Average fiber volume fraction, $(V_f)_{avg}$, is taken as 50%. Transverse variation of these elastic constants in a unidirectional laminate is shown in Figs 3(a)–(d).

Unidirectional laminates

A unidirectional laminate is constructed by 0° laminae only such that fibers in all laminae are oriented along the X-axis (Fig. 1), i.e. in the direction of axial compression. The stress–strain relations can be written as

$$\begin{Bmatrix} \sigma_x \\ \sigma_y \\ \sigma_{xy} \end{Bmatrix} = \begin{bmatrix} Q_{11} & Q_{12} & 0 \\ Q_{12} & Q_{22} & 0 \\ 0 & 0 & Q_{33} \end{bmatrix} \begin{Bmatrix} \varepsilon_x \\ \varepsilon_y \\ \varepsilon_{xy} \end{Bmatrix}, \tag{20}$$

where

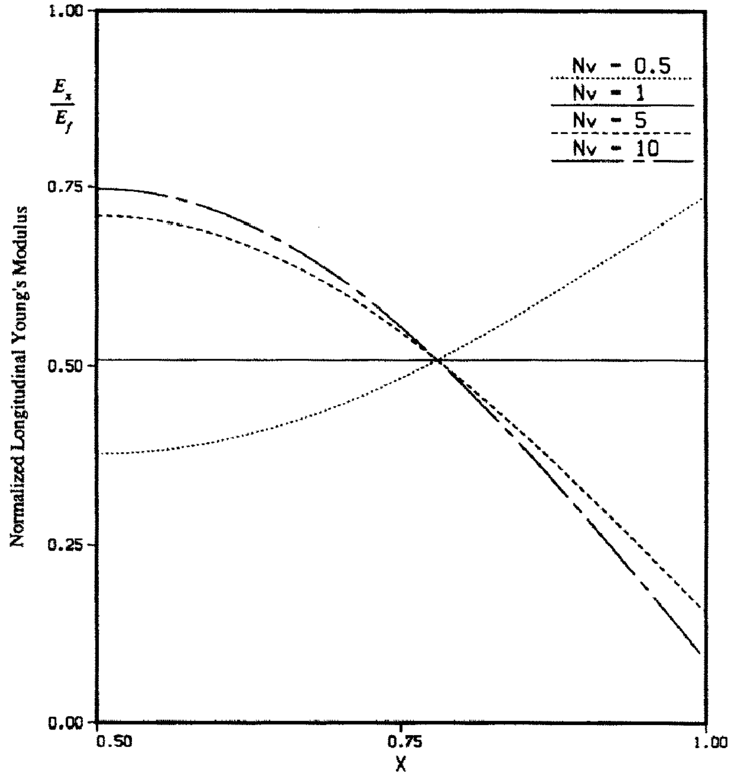

(a)

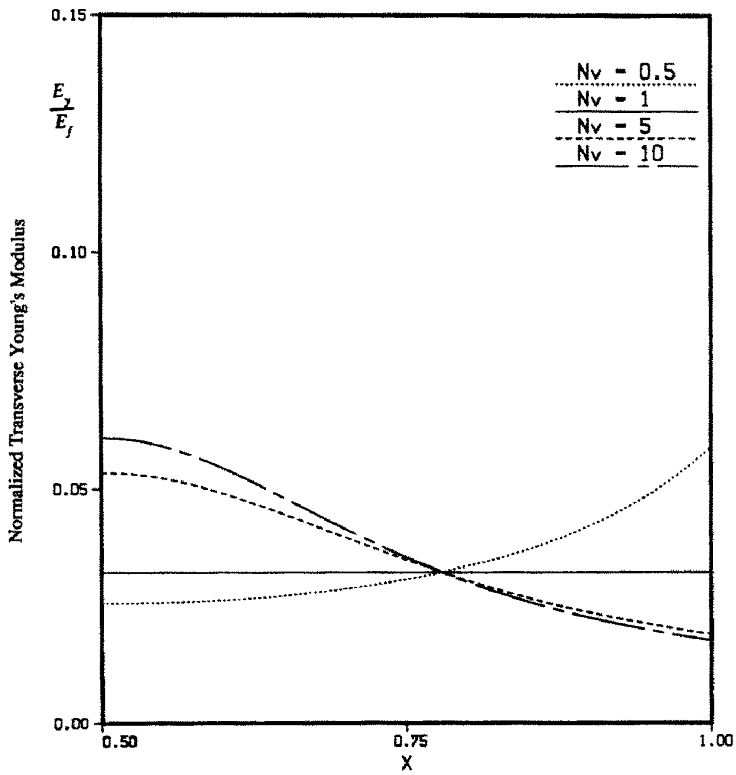

(b)

Fig. 3. Transverse variation of elastic constants: (a) E_x; (b) E_y; (c) ν_{xy}; (d) G_x.

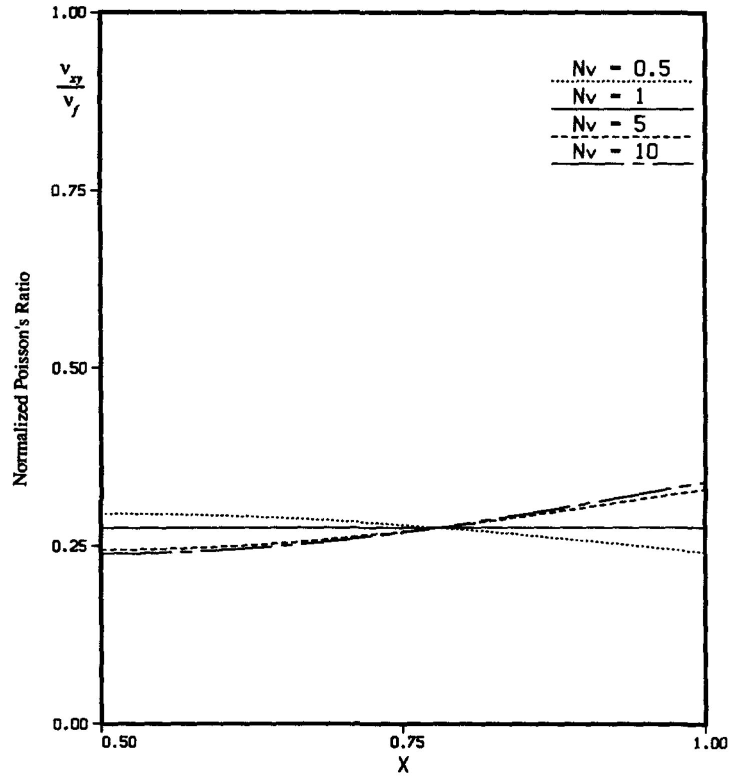

(c)

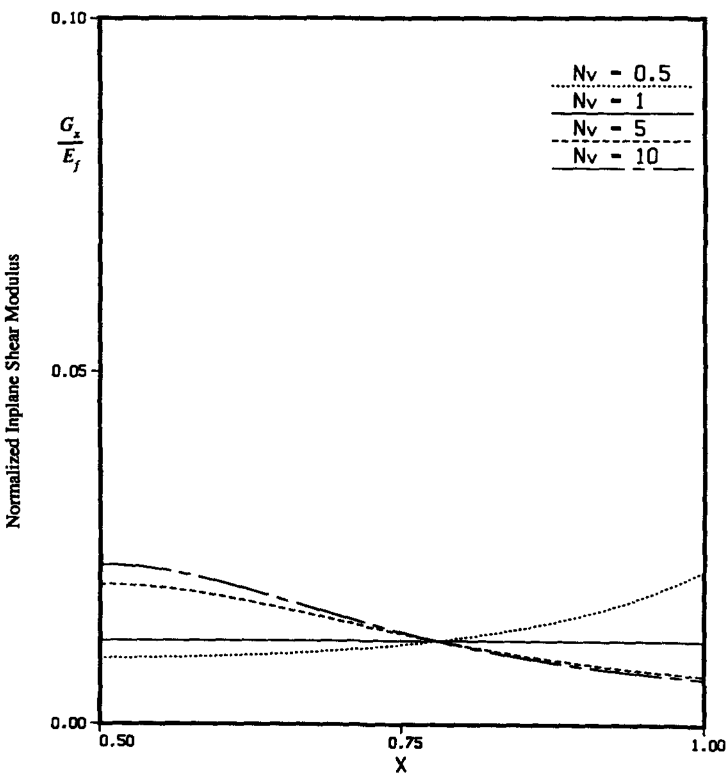

(d)

Fig. 3. *continued.*

$$Q_{11} = \frac{E_x}{d}, \quad Q_{12} = \frac{v_{xy}E_y}{d}, \quad Q_{22} = \frac{E_y}{d}, \quad Q_{33} = G_{xy}, \quad d = 1 - v_{xy}v_{yx} \quad \text{and} \quad v_{yx} = \frac{v_{xy}E_y}{E_x}. \tag{21}$$

Compliance and bending stiffness matrices, C_{ij} and D_{ij}, respectively, are defined as

$$C_{ij} = Q_{ij}^{-1} \quad \text{and} \quad D_{ij} = \frac{Q_{ij}t^3}{12}. \tag{22}$$

Cross-ply laminates

A cross-ply laminate consists of N_P unidirectionally reinforced orthotropic laminae with principal material directions alternatingly oriented at 0 and 90° to the laminate coordinate axes. Thus, the laminate consists of two distinct, 0 and 90°, ply-groups. The thickness of the laminae in a group are identical but not necessarily the same as in the other group. As a special case, a symmetric cross-ply laminate, with N_P odd, is considered where fiber orientations of odd and even numbered layers are 0 and 90°, respectively (Fig. 4). Here, the ratio of the total thickness of 0° odd numbered layers to the total thickness of 90° even numbered layers, C_P, also known as the cross-ply ratio, is an important geometrical parameter. The stiffness matrix Q^c_{ij}, is given by (Jones, 1975):

$$Q^c_{11} = \frac{(C_P + C_T)}{1 + C_P} Q_{11}, \quad Q^c_{22} = \frac{(1 + C_P C_T)}{1 + C_P} Q_{11},$$

$$Q^c_{12} = Q_{12}, \quad Q^c_{33} = tQ_{33}, \quad Q^c_{13} = Q^c_{23} = 0. \tag{23}$$

The bending stiffness is defined by

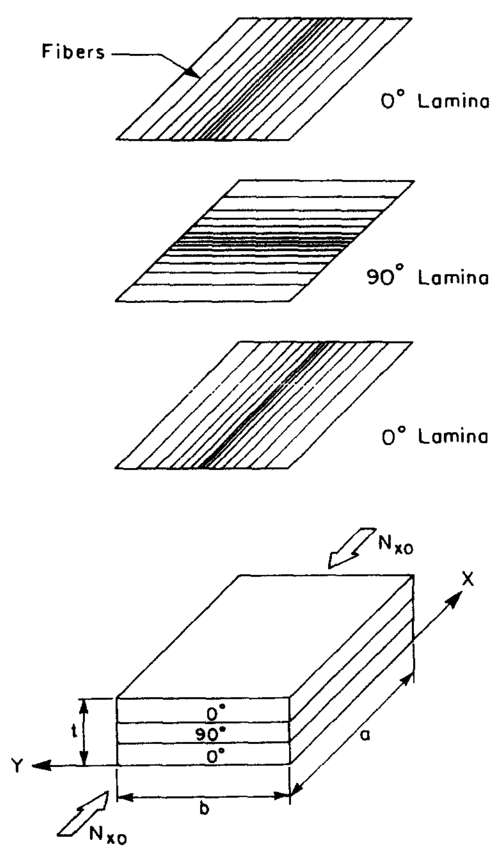

Fig. 4. Inhomogeneous cross-ply laminate ($N_v > 1$).

$$D_{11} = [(C_T - 1)C_B + 1]Q_{11}\frac{t^3}{12}, \quad D_{22} = [(1 - C_T)C_B + C_T]Q_{11}\frac{t^3}{12},$$

$$D_{12} = Q_{12}\frac{t^3}{12}, \quad D_{33} = Q_{33}\frac{t^3}{12}, \quad D_{13} = D_{23} = 0, \tag{24}$$

where

$$C_B = \frac{1}{(1+C_P)^3} + \frac{C_T(N_P - 3)[C_T(N_P - 1) + 2(N_P + 1)]}{(N_P^2 - 1)(1 + C_T)^3} \quad \text{and} \quad C_T = \frac{Q_{22}}{Q_{11}}.$$

PREBUCKLING STRESS ANALYSIS

The prebuckling stress state in an inhomogeneous plate under in-plane forces is derived by a stress-function (complementary energy) formulation combined with the Ritz method. The stress function can be assumed to be in the following series form

$$F(X, Y) = F_P + \sum_{m=1}^{N}\sum_{n=1}^{N} A_{mn}\phi_m(X)\psi_n(Y), \tag{25}$$

where F_P is the particular solution which is due to applied stresses at the plate boundaries. For example, in the case of uniaxial compression, $\sigma_x = \sigma_{x0}$ at $(X = 0, 1)$, a particular solution for the stress function can be assumed as $F_P = \frac{1}{2}\sigma_{x0}b^2Y^2$. $\phi_m(X)$ and $\psi_n(Y)$ are orthogonal polynomial sequences which, at least, satisfy the geometrical boundary conditions in X and Y directions, respectively. These polynomials are generated by a Gram–Schmidt method for given boundary conditions, the detail of which can be found elsewhere (Bhat, 1985; Pandey and Sherbourne, 1991). Using eqn (5), the in-plane stress field can be given as

$$\sigma_x = \frac{1}{b^2}\left[F_{P,yy} + \sum_{m=1}^{N}\sum_{n=1}^{N} A_{mn}\phi_m(X)\psi_{n,yy}(Y)\right],$$

$$\sigma_y = \frac{1}{a^2}\sum_{m=1}^{N}\sum_{n=1}^{N} A_{mn}\phi_{m,xx}(X)\psi_n(Y),$$

$$\sigma_{xy} = \frac{-1}{ab}\sum_{m=1}^{N}\sum_{n=1}^{N} A_{mn}\phi_{m,x}(X)\psi_{n,y}(Y). \tag{26}$$

The incremental potential energy of an inhomogeneous plate under plane-stress conditions (Bassily and Dickinson, 1977) is given by

$$U_i = \frac{1}{2}\int_0^1\int_0^1 [C_{11}\sigma_x^2 + C_{22}\sigma_y^2 + 2C_{12}\sigma_x\sigma_y + C_{33}\sigma_{xy}^2]\,dX\,dY, \tag{27}$$

which can be written in terms of the stress function as

$$U_i = \frac{1}{2a^4}\int_0^1\int_0^1 [\beta^4C_{11}(F_{,yy})^2 + C_{22}(F_{,xx})^2 + 2\beta^2C_{12}F_{,yy}F_{,xx} + \beta^2C_{33}(F_{,xy})^2]\,dX\,dY. \tag{28}$$

The final expression for the potential energy, U_i, can be written by substituting from eqns (25) into eqn (28). Following the standard Rayleigh–Ritz method, minimization of the potential function, U_i, with respect to the coefficients A_{mn} leads to the following system of linear simultaneous equations

$$\sum_{m=1}^{N}\sum_{n=1}^{N}[H_{mnij}]\{A_{mn}\} = -\{P_{ij}\}. \tag{29}$$

The in-plane stiffness matrix, H_{mnij}, may be written

$$H_{mnij} = R_{mi}^{(2,2)}\{C_{22}S_{nj}^{(0,0)}\}+\beta^2[R_{mi}^{(0,2)}\{C_{12}S_{nj}^{(2,0)}\}+R_{mi}^{(2,0)}\{C_{12}S_{nj}^{(0,2)}\}]+\beta^4R_{mi}^{(0,0)}\{C_{11}S_{nj}^{(2,2)}\} +\beta^2R_{mi}^{(1,1)}\{C_{33}S_{nj}^{(1,1)}\} \tag{30}$$

and the loading vector, P_{ij}, is given as

$$P_{ij} = \beta^4F_{P_{,yy}}R_i^{(0)}\{C_{11}S_j^{(2)}\}+F_{P_{,xx}}R_i^{(2)}\{C_{22}S_j^{(0)}\}+\beta^2F_{P_{,xy}}R_i^{(1)}\{C_{33}S_j^{(1)}\} +\beta^2(F_{P_{,xx}}R_i^{(0)}\{C_{12}S_j^{(2)}\}+F_{P_{,yy}}R_i^{(2)}\{C_{12}S_j^{(0)}\}). \tag{31}$$

The integral terms are denoted by the following compact notation

$$R_{mi}^{(r,s)} = \int_0^1 \frac{d^r\phi_m(X)}{dX^r}\frac{d^s\phi(X)}{dX^s}dX \quad \text{and} \quad S_{nj}^{(r,s)} = \int_0^1 \frac{d^r\psi_n(Y)}{dY^r}\frac{d^s\psi(Y)}{dY^s}dY,$$

$$R_i^{(r)} = \int_0^1 \frac{d^r\phi_m(X)}{dX^r}dX \quad \text{and} \quad S_j^{(r)} = \int_0^1 \frac{d^r\psi_m(Y)}{dY^r}dY,$$

$$\{C_{kl}S_{nj}^{(r,s)}\} = \int_0^1 C_{kl}(Y)\frac{d^r\psi_n(Y)}{dY^r}\frac{d^s\psi_j(Y)}{dY^s}dY. \tag{32}$$

The system of equations can be solved for coefficients, A_{mn}, and thus the prebuckling stress state can be defined.

BUCKLING

The potential energy of a rectangular orthotropic plate (Fig. 1) under in-plane loading at incipient buckling is given as follows (Whitney, 1987)

$$U_B = \frac{1}{2a^4}\int_0^1\int_0^1 \{D_{11}(W_{,xx})^2+2D_{12}\beta^2W_{,xx}W_{,yy}+D_{22}\beta^4(W_{,yy})^2 +4D_{33}\beta^2(W_{,xy})^2+a^2t[\sigma_x(W_{,x})^2+\beta^2\sigma_y(W_{,y})^2+2\beta\sigma_{xy}W_{,xy}\}\,dX\,dY. \tag{33}$$

Here, $W(x,y)$ is the normalized out-of-plane displacement and D_{ij}, $i,j=1,\ldots,3$, are the bending stiffnesses derived by applying Kirchhoff's plate theory to orthotropic laminates (Jones, 1975). The displacement functions are assumed in the following separable form:

$$W(X,Y) = \sum_{m=1}^{N}\sum_{n=1}^{N} B_{mn}\phi_m(X)\psi_n(Y), \tag{34}$$

where $\phi_m(X)$ and $\psi_n(Y)$ are orthogonal polynomial sequences which, at least, satisfy the geometrical boundary conditions in X and Y directions, respectively. The assumed displacement functions from eqn (34) and prebuckling stresses from eqn (26) are substituted in eqn (33). Following the standard Rayleigh–Ritz method, minimization of the potential function, U_B, with respect to the coefficients B_{mn} leads to the following generalized eigenvalue problem

$$\sum_{m=1}^{N}\sum_{n=1}^{N}[E_{mnij}]\{B_{mn}\} = \lambda a^2 t[G_{mnij}]\{B_{mn}\}. \tag{35}$$

The stiffness matrix, E_{mnij}, may be written as

$$E_{mnij} = R_{mi}^{(2,2)}\{D_{11}S_{nj}^{(0,0)}\}+\beta^2\left(R_{mi}^{(0,2)}\{D_{12}S_{nj}^{(2,0)}\}+R_{mi}^{(2,0)}\{D_{12}S_{nj}^{(0,2)}\}\right) + \beta^4 R_{mi}^{(0,0)}\{D_{22}S_{nj}^{(2,2)}\}+4\{\beta^2 R_{mi}^{(1,1)}\}\{D_{33}S_{nj}^{(1,1)}\}. \tag{36}$$

Terms $\{D_{kl}S_{nj}^{(r,s)}\}$ are defined in the same way as $\{C_{kl}S_{nj}^{(r,s)}\}$ in eqn (32). The geometric stiffness matrix, G_{mnij}, is given as

$$G_{mnij} = \left\{\frac{F_{\mathrm{P},yy}}{b^2} R_{mi}^{(1,1)}S_{nj}^{(0,0)}+\beta^2\frac{F_{\mathrm{P},xx}}{a^2} R_{mi}^{(0,0)}S_{nj}^{(1,1)}+\beta\frac{F_{\mathrm{P},xy}}{(-ab)}\left(R_{mi}^{(0,1)}S_{nj}^{(1,0)}+R_{mi}^{(1,0)}S_{nj}^{(0,1)}\right)\right\}$$
$$+\sum_{K=1}^{M}\sum_{L=1}^{N} A_{KL}\left\{\frac{1}{b^2}R_{Kmi}^{(0,1,1)}S_{Lnj}^{(2,0,0)}+\frac{\beta^2}{a^2}R_{Kmi}^{(2,0,0)}S_{Lnj}^{(0,1,1)}\right.$$
$$\left.+\frac{\beta}{(-ab)}R_{Kmi}^{(1,0,1)}S_{Lnj}^{(1,1,0)}+\frac{\beta}{(-ab)}R_{Kmi}^{(1,1,0)}S_{Lnj}^{(1,0,1)}\right\}. \tag{37}$$

The following compact notation is used to define three term integrations

$$R_{Kmi}^{(r,s,t)} = \int_0^1 \frac{\mathrm{d}^r\phi_K(X)}{\mathrm{d}X^r}\frac{\mathrm{d}^s\phi_m(X)}{\mathrm{d}X^s}\frac{\mathrm{d}^t\phi_i(X)}{\mathrm{d}X^t} \quad \text{and} \quad S_{Lnj}^{(r,s,t)} = \int_0^1 \frac{\mathrm{d}^r\psi_L(Y)}{\mathrm{d}Y^r}\frac{\mathrm{d}^s\psi_n(Y)}{\mathrm{d}Y^s}\frac{\mathrm{d}^t\psi_j(Y)}{\mathrm{d}Y^t}. \tag{38}$$

Uniaxial compression

In the case of uniaxial compression, $\sigma_x = \sigma_{x0}$ at $(X = 0, 1)$, a particular solution for the stress function can be assumed to be

$$F_\mathrm{P} = \tfrac{1}{2}\sigma_{x0}b^2Y^2 \quad \text{so that} \quad F_{\mathrm{P},yy} = \sigma_{x0}b^2 \quad \text{and} \quad F_{\mathrm{P},xx} = F_{\mathrm{P},xy} = 0. \tag{39}$$

Coefficients A_{mn}, defining the prebuckling stress field in eqn (26) can be obtained from the following specialized form of eqn (29):

$$\sum_{m=1}^{N}\sum_{n=1}^{N}[H_{mnij}]\{A_{mn}\} = -\sigma_{x0}a^2\{P_{ij}^x\}, \quad \text{where} \quad P_{ij}^x = \beta^2 R_i^{(0)}\{C_{11}S_j^{(2)}\}+R_i^{(2)}\{C_{12}S_j^{(0)}\}. \tag{40}$$

It is clear that $\sigma_{x0}a^2$ is the common multiplying factor for coefficients, A_{mn}. The uniaxial buckling problem can be defined from eqn (35) as

$$\sum_{m=1}^{N}\sum_{n=1}^{N}[E_{mnij}]\{B_{mn}\} = \lambda\sigma_{x0}a^2t[G_{mnij}^x]\{B_{mn}\}$$

where

$$G^{x}_{mnij} = R^{(1,1)}_{mi} S^{(0,0)}_{nj} + \beta^2 \sum_{K=1}^{M} \sum_{L=1}^{N} A_{KL} \{ R^{(0,1,1)}_{Kmi} S^{(2,0,0)}_{Lnj} + R^{(2,0,0)}_{Kmi} S^{(0,1,1)}_{Lnj} - R^{(1,0,1)}_{Kmi} S^{(1,1,0)}_{Lnj} - R^{(1,1,0)}_{Kmi} S^{(1,0,1)}_{Lnj} \}. \quad (41)$$

Pure shear

In this case, a particular solution for the stress function can be assumed as

$$F_P = -\sigma_{xy0} abXY \quad \text{so that} \quad F_{P,xy} = -\sigma_{xy0} ab \quad \text{and} \quad F_{P,xx} = F_{P,yy} = 0. \quad (42)$$

In-plane stress analysis involves solution of the following system of equations:

$$\sum_{m=1}^{N} \sum_{n=1}^{N} [H_{mnij}]\{A_{mn}\} = \sigma_{xy0} a^2 \{P^{xy}_{ij}\}, \quad \text{where} \quad P^{xy}_{ij} = \beta R^{(1)}_{i} \{C_{33} S^{(1)}_{j}\}. \quad (43)$$

while the buckling problem can be defined by eqn (35) after substituting appropriately from (42) into (37).

Boundary conditions: further remarks

In this section, the analogy between boundary conditions in bending and stretching is further explained by a specific example of a uniaxially compressed plate. The stress function, F, and displacement, W, respectively, are assumed in the series form shown by eqns (25) and (34).

Clamped supports (bending). Coordinate functions for W are chosen to satisfy B.C.s (13) such that, $\phi_m(X) = \phi_{m,x}(X) = 0$ at $X = 0$. In-plane stresses, as defined in eqn (26), provide the following conditions also referred to as free B.C.,

$$\sigma_x = \sigma_{x0} \quad \text{and} \quad \sigma_{xy} = 0 \quad at \quad X = 0.$$

Simple supports (bending). Coordinate functions are chosen to ensure, $\sigma_m(X) = \phi_{m,xx}(X) = 0$ at $X = 0$. From eqn (26), at the edge $X = 0$,

$$\sigma_x = \sigma_{x0}, \quad \sigma_y = 0 \quad \text{and} \quad \varepsilon_{xy} \neq 0 \text{ which refer to a laterally restrained edge.}$$

RESULTS AND DISCUSSION

In-plane stress and buckling solutions for two loading conditions, *viz.* uniaxial compression and pure shear, are discussed. A typical calculation of buckling loads consists of two steps. Firstly, an accurate prebuckling stress field is derived using eqn (29) and, incorporated in the second step of out-of-plane buckling analysis as shown by eqn (35). The duality between the plane stress and bending problems provides a concise and convenient analytical framework but it should be clear that such duality is exploited for theoretical convenience and may be far removed from practical situations. For example, a clamped plate (CCCC) in bending is assumed to have free in-plane edge conditions (FFFF) that may not be true in practice where a more complex combination of in-plane and out-of-plane boundary conditions is likely to exist than one governed by the duality as discussed. Nevertheless, the present approach allows one to obtain benchmark solutions and, also, highlights the potential of inhomogeneous, composite laminates for improved buckling behavior. The boundary conditions (B.C.) are denoted by the letter S for simple, C for clamped and F for free along the four edges in the following order, $x = 0$, $x = a$ (loaded edges), $y = 0$ and $y = b$ (unloaded edges). Thus, support conditions denoted by SSCC means that loaded edges, $x = 0$ and a, are simply supported and unloaded edges, $y = 0$ and b, are clamped.

In-plane stress analysis

The in-plane stress solutions for axially compressed square plates with parabolic fiber distribution and all four edges free, are reported in Figs 5(a)–(c). These results are in close agreement with those obtained by Martin and Leissa (1989) who adopted a displacement version of the Ritz method treating in-plane displacements, u and v, as variables which is contrary to the proposed technique where stress function, F, is the only variable. A stress concentration factor of $\sigma_x/\sigma_{x0} = 1.19$, as reported by Martin and Leissa (1989), is also verified.

Figures 6 and 7 show distributions of stresses, σ_x at $X = 0.5$, σ_y at $Y = 0.5$ and σ_{xy} at $X = 0.75$, plotted for three sinusoidal fiber distributions corresponding to $N_v = 0.5$, 5 and 10. Only one half of the distribution is shown because of symmetry. Solutions are fairly rapidly converging and the results are obtained for $N = 9$ terms.

In the case of uniaxial compression, stresses, σ_x, σ_y and σ_{xy}, in a FFFF unidirectional (UD) laminate are plotted in Figs 6(a)–(c), respectively. A stress concentration of $\sigma_x/\sigma_{s0} \approx 1.1$ is observed which is less severe compared to parabolic fiber distribution. In general, σ_y and σ_{xy} are quite small. Convergence behavior of uniaxial stress, σ_x, is presented in Tables 2(a) and (b) for $N_v = 0.5$ and 5, respectively. In Tables 2(a) and (b) out-of-plane boundary conditions are denoted inside brackets. Stress values at $X = 0.5$ and Y varying from 0 to 0.5 are calculated for three edge conditions, *viz.* FFFF, SSFF and SSSS. Increasing the number of polynomial terms from five to nine leads to a fairly good convergence especially at points located in the plate interior, e.g. $X = 0.5$ and $Y = 0.2$–0.5. In general, stress convergence in FFFF and SSFF plates is faster than the SSSS plate. Also, $N_v = 0.5$ leads to a better convergence characteristic than $N_v = 5$. Stresses in a FFFF cross-ply laminate ($N_P = 3$) with $C_P = 1$ are plotted in Fig. 7. Uniaxial stress, σ_x, is largely uniform over the width. It is noteworthy that $\sigma_x/\sigma_{x0} \approx 1$ for $N_v = 0.5$. It should be noted that σ_y is more pronounced in a cross-ply compared to a unidirectional laminate as expected due to the presence of 90° plies. Shear stresses are almost insignificant in both the U.D. and cross-ply laminates. Edge effects, which are quite pronounced, are less likely to affect buckling solutions as the plate is supported at the edges such that out-of-plane displacements are zero.

Numerical results indicate that in the case of U.D. as well as cross-ply laminates under pure applied shear, the prebuckling stress state is one of uniform shear throughout, such that, $\sigma_{xy} = \sigma_{xy0}$ and $\sigma_x = \sigma_y = 0$. It is numerically verified for simply-supported and free B.C.s and their combinations.

Buckling

The major part of the study is devoted to the computation of uniaxial and shear buckling coefficients, N_x and N_{xy}, respectively, for various B.C.s and fiber distributions for unidirectional and cross-ply laminates with $C_p = 2$ and 1. It should be stressed, once again, that the computation of buckling coefficients is based on accurate prebuckling stress distributions which properly take into account material inhomogeneity. Presently, only three layered cross-ply laminates ($N_P = 3$) are considered, the cross-section of which, is shown in Fig. 4. In all cases, results are obtained for square ($a/b = 1$) laminates by taking $N = 6$ in both the plane-stress and buckling problems. Buckling coefficients are also obtained by assuming a uniform prebuckling state represented by $\sigma_x = \sigma_{x0}$ and $\sigma_y = \sigma_{xy} = 0$ in uniaxial compression, and, $\sigma_{xy} = \sigma_{xy0}$ and $\sigma_x = \sigma_y = 0$ in pure shear. These solutions are denoted by a superscript "u", e.g., N_x^u and N_{xy}^u.

The uniaxial buckling coefficients, $N_x = \sigma_{x0}a^2t/D_f$, are tabulated in Tables 3(a)–(c). Here, $D_f = E_f t^3/12$. The increase in buckling load when $N_v = 5$ over uniform fiber distribution, i.e. $N_v = 1$, is shown in Table 4. As a general rule, a higher fiber concentration at the centre compared to the edges ($N_v \geqslant 5$) results in an increase in the buckling load. The strain energy density near the central region is usually higher than near the edges and, hence, location of higher fiber content in this region is intuitively appealing (Sherbourne and Pandey, 1991) and, also, follows the notion of Spiller and Levy (1990) regarding the optimal thickness distribution. From Tables 3(b) and (c), it can be seen that cross-ply arrangements increase buckling loads for plates with loaded edges being simply supported,

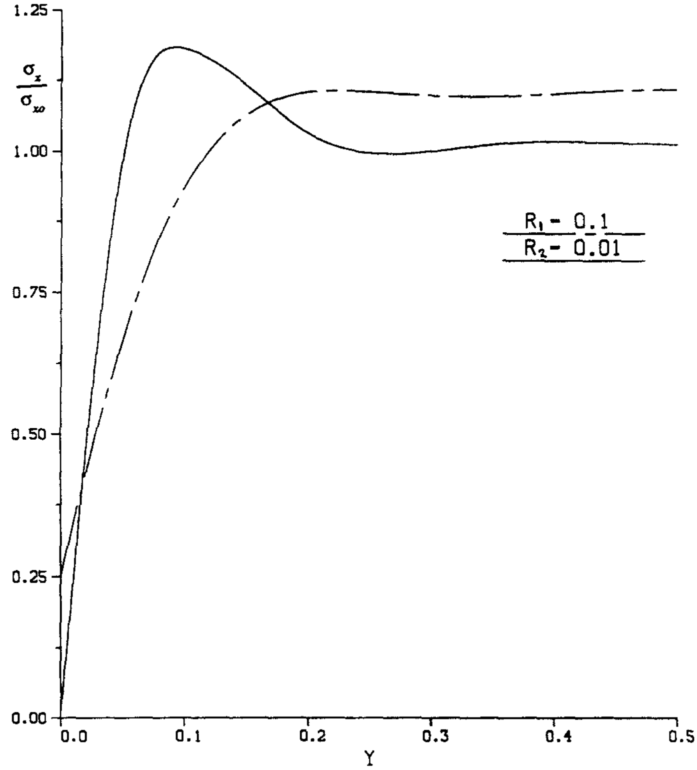

(a)

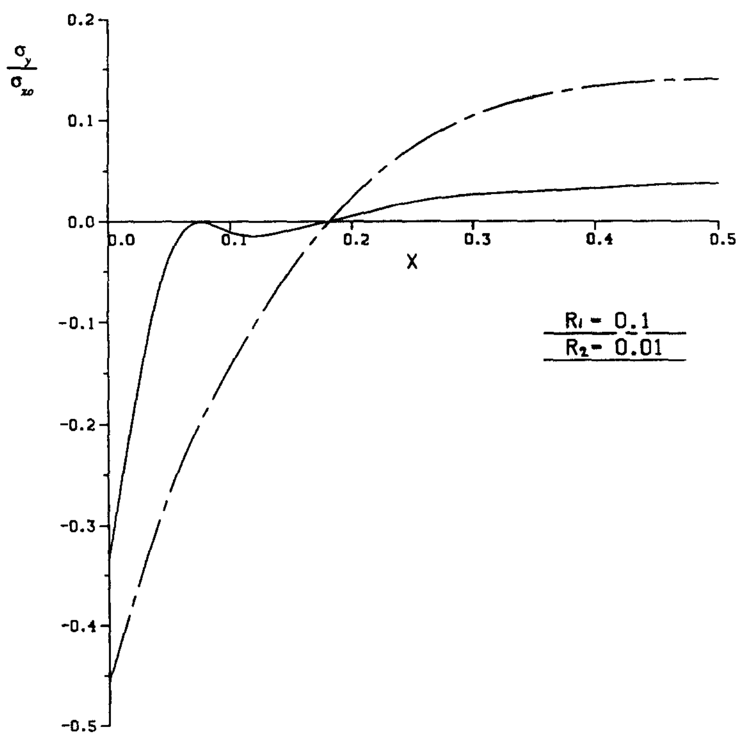

(b)

Fig. 5. In-plane stresses with parabolic fiber distribution: (a) σ_x at $X = 0.5$; (b) σ_y at $Y = 0.5$; (c) σ_{xy} at $X = 0.75$.

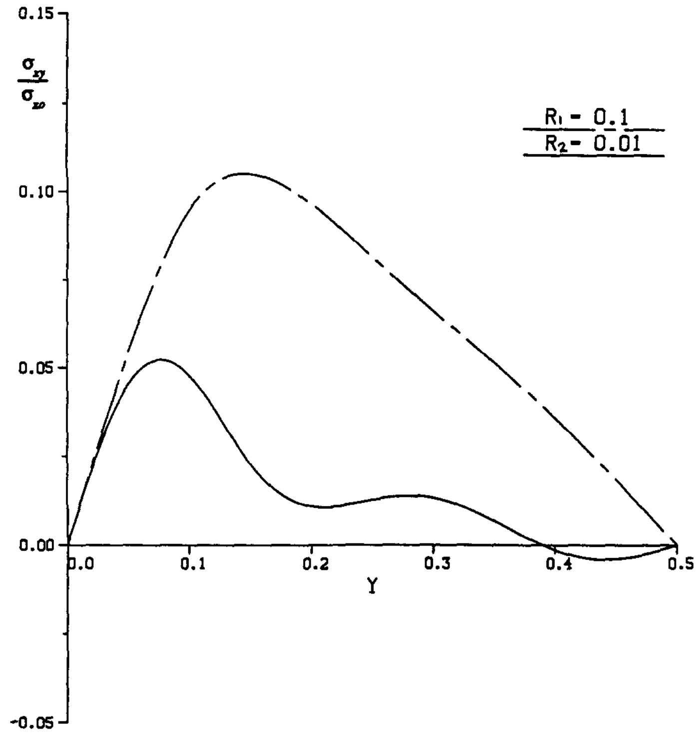

(c)

Fig. 5. *continued.*

e.g. SSSS, SSCC, and decrease when loaded edges are clamped, e.g. CCCC, CCSS. Cross-ply laminates with simply-supported loaded edges have slightly higher buckling loads than 0° laminates and the reverse is true when loaded edges are clamped. It suggests that cross-ply construction is not effective when loaded edges are clamped. It is interesting to note from Table 3(c) that the buckling behavior of SSCC cross-ply laminates with $C_P = 1$ is rather exceptional, since higher fiber concentration at the edges ($N_v = 0.5$) compared to the middle increases the buckling load. The numerical results indicate that, for the range of the parameter N_v and boundary conditions considered herein, the error incurred in computing buckling coefficients in accordance with the assumption of uniform prebuckling is not too large and the qualitative nature of the solutions is well preserved. It must be stressed, however, that such a conclusion follows a detailed parametric study, and its generalization to other B.C.s and aspect ratios is cautioned. Convergence of N_x is presented in Tables 5(a) and (b) for U.D. and cross-ply ($C_P = 1$) laminates with CCCC and SSCC edges. In fact, for all cases of fiber distributions and B.C.s, the buckling load converged monotonically and could be accurately approximated by $N = 6$ terms in the polynomial series.

Uniaxial buckling loads of simply-supported 0° laminates with a parabolic fiber distribution given by eqn (18) are presented in Table 6 together with those obtained by Leissa and Martin (1990). The results obtained by the two formulations appear to be in good agreement. Minor discrepancies may be attributed to the fact that in-plane boundaries, in the present case, are taken to be simply supported as opposed to the free boundaries assumed by Leissa and Martin (1990). The properties of composite materials in Table 6 are taken from the previous study (Leissa and Martin, 1990).

Shear buckling coefficients, $N_{xy} = \sigma_{xy}a^2t/D_f$, are tabulated in Tables 6(a)–(c). The increase in buckling load when $N_v = 5$ over uniform fiber distribution, i.e. $N_v = 1$, is shown in Table 7. The buckling load increases when fiber is concentrated at the centre, the increase being maximum for a SSCC, 0° laminate. Cross-ply is more effective in shear buckling than unidirectional laminates because of the orientation of fibers perpendicular to the shear direction. Even in the case of uniform fiber distribution, $N_v = 1$, the shear buckling load of a CCCC cross-ply ($C_P = 1$) is 35% higher than that of an equal volume unidirectional (0°)

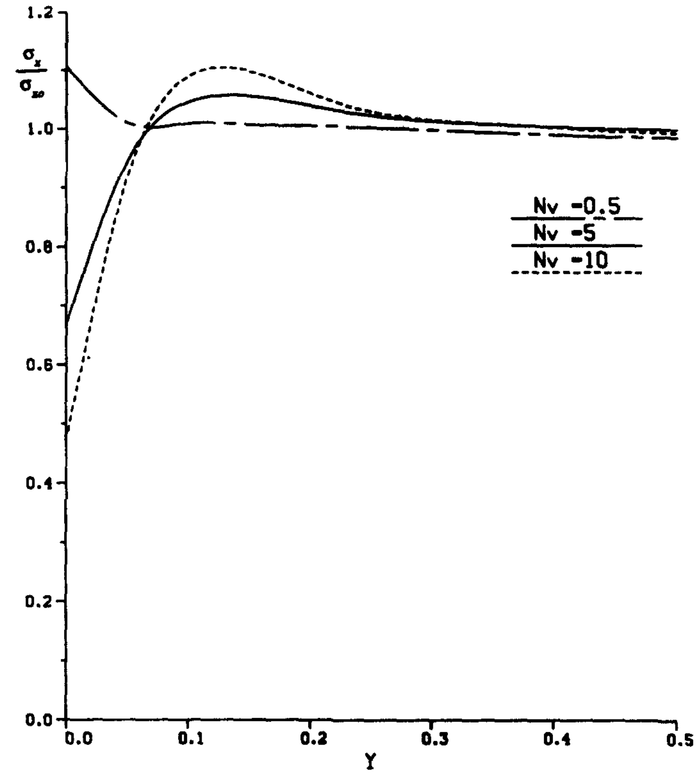

(a)

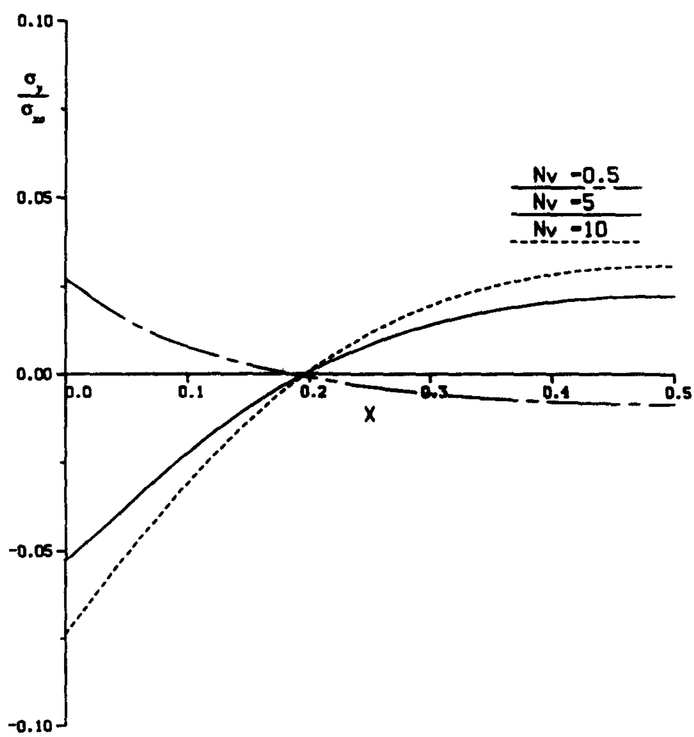

(b)

Fig. 6. In-plane stresses with sinusoidal fiber distribution: (a) σ_x at $X = 0.5$; (b) σ_y ast $Y = 0.5$; (c) σ_{xy} at $X = 0.75$.

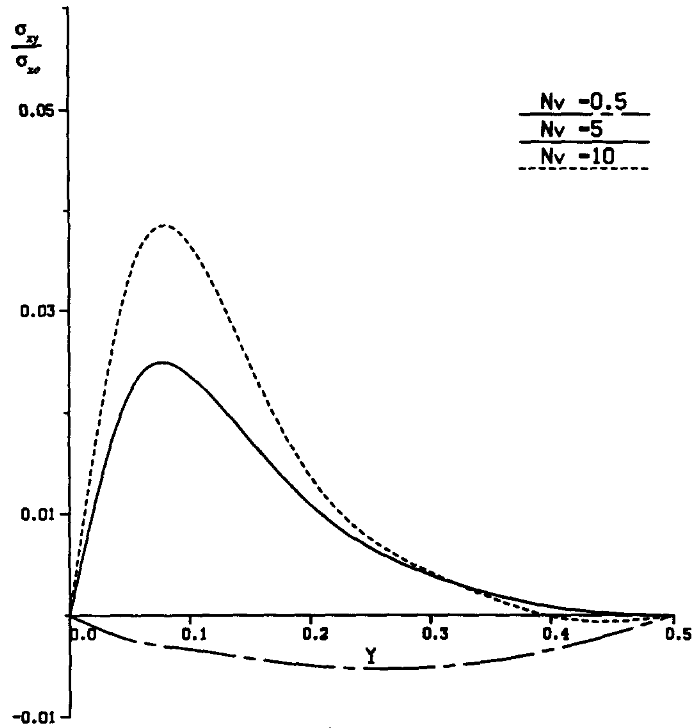

(c)

Fig. 6. *continued.*

laminate. Because of uniform prebuckling under applied shear, buckling coefficients, N_{xy} and N^{u}_{xy}, are identical, i.e. $N_{xy} = N^{u}_{xy}$, for all the cases considered.

Comparison with Leissa and Martin (1990)

Leissa and Martin (1990) have studied buckling and vibration of simply-supported, unidirectional (0°) laminae and variable fiber spacing defined by various types of distribution functions. The plane stress solutions were obtained by adopting a displacement version of the Ritz method and employing series expansions for in-plane displacements, u and v. In the present version of the Ritz analysis, stress function, F, is the only variable as compared to the displacement formulation with two unknowns, u and v, which is computationally advantageous. In the buckling analysis, the assumption of simply-supported boundaries allowed the use of the Fourier sine series, $\sin m\pi X \sin n\pi Y$, as the displacement function which simplified the evaluation of the displacement derivatives and the energy integrals. It is also clear that the plane stress and buckling analyses are treated independently resulting in increased computational efforts. This approach may appear to be suitable in the particular case of simply-supported plates but its extension to other general boundary conditions is believed to be complicated, at least, from a computational point of view. In specific terms, the evaluation of work done by in-plane forces at incipient buckling, that is the load matrix, G_{mnij}, in eqn (35), would be very difficult when different sets of functions, for in-plane and out-of-plane displacements, are employed.

It is proposed, therefore, to combine the plane stress and the buckling analysis using the classical bending–stretching analogy which allows the use of the same set of displacement functions in the two stages. This key feature has greatly simplified the computational formulation of the Ritz method. Orthogonal polynomials are convenient means for handling simple and clamped B.C.s and their combinations. Also, the formulation provides a general framework to accommodate axial as well as shear loading.

The two formulations are compared in Table 8 where uniaxial buckling loads of simply-supported 0° laminates with a parabolic fiber distribution given by eqn (18) are presented together with those obtained by Leissa and Martin (1990). The results obtained by the two formulations appear to be in good agreement. Minor discrepancies may be attributed to

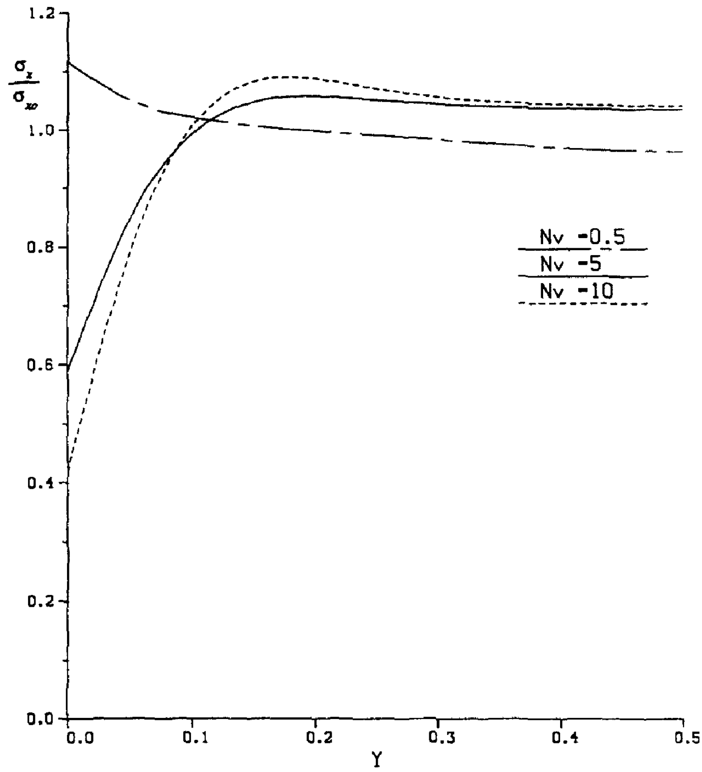

(a)

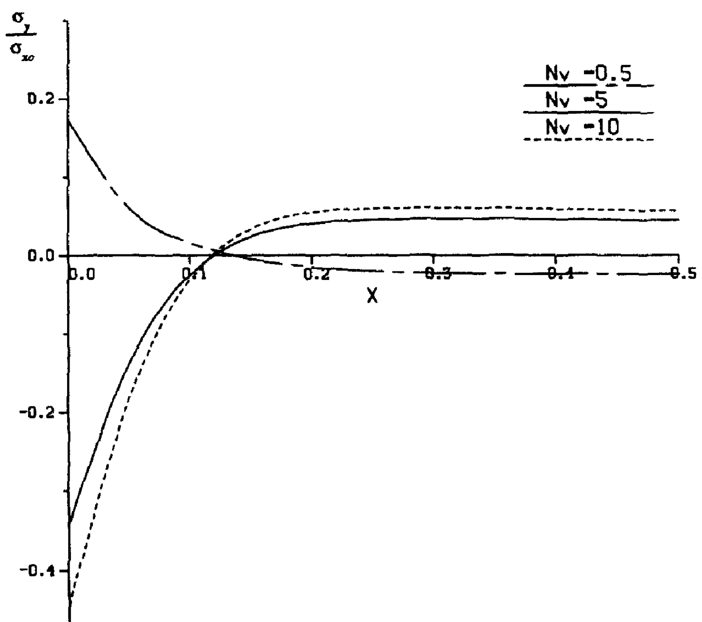

(b)

Fig. 7. In-plane stresses in a cross-ply laminate ($C_P = 1$): (a) σ_x at $X = 0.5$; (b) σ_y at $Y = 0.5$; (c) σ_{xy} at $X = 0.75$.

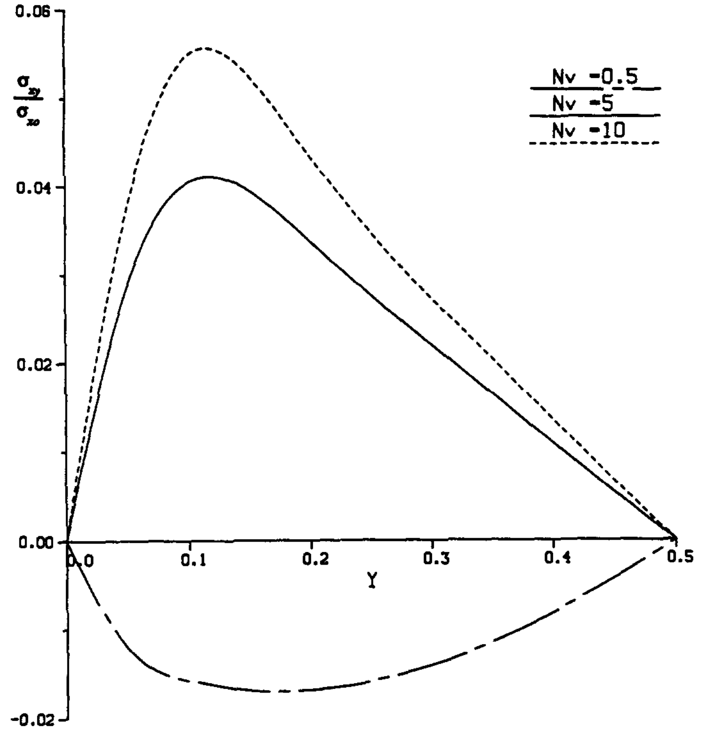

(c)

Fig. 7. *continued.*

the fact that in-plane boundaries, in the present case, are taken to be simply supported as opposed to free boundaries assumed by Leissa and Martin (1990). The results shown in Table 8 are based on the same composite material properties as used in the previous study (Leissa and Martin, 1990).

CONCLUSION

The use of composite materials in the fabrication of structural components significantly widens the range of possible designs open to engineers. Cases involving non-uniform fiber distribution are much more difficult to tackle and have thus received much less attention

Table 2. Convergence of σ_x in a 0° lamina

(a) For $N_v = 0.5$

	FFFF (CCCC)			SSFF (SSCC)			SSSS (SSSS)		
Y	$N=5$	$N=7$	$N=9$	$N=5$	$N=7$	$N=9$	$N=5$	$N=7$	$N=9$
0	1.015	1.0142	1.0161	0.99294	0.99448	0.99701	0.25448	−0.02027	−0.04242
0.1	1.0083	1.0083	1.0086	1.0115	1.0108	1.0115	0.77109	0.84204	0.8471
0.2	1.0049	1.0047	1.00456	1.0097	1.0096	1.0092	1.0132	1.0123	1.001
0.3	0.99766	0.99786	0.99787	0.99898	0.99939	0.9994	1.0444	0.99736	1.0057
0.4	0.98968	0.98974	0.98986	0.98852	0.98856	0.98879	0.99045	0.99311	0.99577
0.5	0.98626	0.98608	0.9859	0.98434	0.98402	0.98369	0.95875	0.99985	0.99079

(b) $N_v = 5$

	FFFF (CCCC)			SSFF (SSCC)			SSSS (SSSS)		
Y	$N=5$	$N=7$	$N=9$	$N=5$	$N=7$	$N=9$	$N=5$	$N=7$	$N=9$
0	0.67113	0.65908	0.66732	0.58711	0.58998	0.59963	0.015726	−0.10522	−0.03017
0.1	1.0441	1.0428	1.0452	1.0188	1.0168	1.0204	0.70797	0.76619	0.75936
0.2	1.0446	1.0413	1.0392	1.0527	1.0524	1.0493	1.0367	1.0111	1.0215
0.3	1.0067	1.0122	1.0131	1.0273	1.0294	1.0308	1.0853	1.0364	1.0268
0.4	1.0021	1.0026	1.0036	1.0241	1.0241	1.0256	1.0189	1.0321	1.0296
0.5	1.0069	1.0013	0.99916	1.0283	1.0262	1.0231	0.97873	1.0326	1.0436

Table 3. Uniaxial buckling coefficients

(a) 0° laminate

	SSSS		CCCC		SSCC		CCSS	
Nv	N_x	N_x^u	N_x	N_x^u	N_x	N_x^u	N_x	N_x^u
0.5	5.3809	5.2545	18.7762	18.5351	6.8921	6.8188	17.9418	17.7535
1	6.0752	6.0061	22.1795	22.1795	7.4194	7.4781	21.1017	21.0452
5	7.1074	7.1206	26.5831	27.1439	8.3918	8.749	24.7478	24.6787
10	7.2831	7.3143	27.1262	27.9418	8.5449	9.0082	25.2068	25.1036
20	7.3749	7.4172	27.3396	28.3576	8.6155	9.1538	25.43	25.3014

(b) Cross-ply laminate ($C_P = 2$)

	SSSS		CCCC		SSCC		CCSS	
Nv	N_x	N_x^u	N_x	N_x^u	N_x	N_x^u	N_x	N_x^u
0.5	5.2681	5.2606	19.2954	18.6926	7.8992	7.6309	18.198	17.3472
1	6.2353	6.0061	22.1525	22.1525	8.1896	8.2046	20.9823	20.4768
5	7.2011	7.138	25.6434	26.8593	8.6803	9.1934	24.5344	24.2808
10	7.3716	7.3386	25.9923	27.5909	8.7129	9.3674	25.0609	24.7957
20	7.4616	7.4455	26.1013	27.9615	8.7142	9.4605	25.3284	25.0426

(c) Cross-ply laminate ($C_P = 1$)

	SSSS		CCCC		SSCC		CCSS	
Nv	N_x	N_x^u	N_x	N_x^u	N_x	N_x^u	N_x	N_x^u
0.5	5.76	5.2636	19.8299	19.026	9.9971	9.558	17.4146	16.2837
1	6.3232	6.0061	22.0407	22.0707	9.9107	9.9257	19.8383	19.1265
5	7.2444	7.1475	24.5136	26.0285	9.5431	10.2338	23.1545	22.9174
10	7.4084	7.3521	24.6507	26.574	9.3481	10.1943	23.6872	23.5042
20	7.4947	7.4612	24.6447	26.8255	9.2111	10.15	23.9618	23.7978

Table 4. Percentage increase in N_x ($N_v = 5$)

Laminate	SSSS	CCCC	SSCC	CCSS
0 Laminate	16.99	19.85	13.11	17.28
Cross-ply ($C_P = 2$)	15.49	15.76	5.99	16.93
Cross-ply ($C_P = 1$)	14.57	11.22	−3.71	16.71

Table 5. Convergence of N_x

(a) 0° laminate

	CCCC			SSCC		
Nv	$N = 5$	$N = 6$	$N = 7$	$N = 5$	$N = 6$	$N = 7$
0.5	18.7762	18.7762	18.7755	6.89207	6.89207	6.89205
1	22.1795	22.1795	22.1794	7.41944	7.41944	7.41948
5	26.5831	26.5831	26.5783	8.39182	8.39182	8.39205
10	27.1262	27.1262	27.113	8.54488	8.54488	8.54521
20	27.3396	27.3396	27.3154	8.61547	8.61547	8.61565

(b) Cross-ply laminate ($C_P = 1$)

	CCCC			SSCC		
Nv	$N = 5$	$N = 6$	$N = 7$	$N = 5$	$N = 6$	$N = 7$
0.5	19.8299	19.8299	19.8305	9.99719	9.99719	9.99668
1	22.0707	22.0707	22.0706	9.91073	9.91073	9.91068
5	24.5136	24.5136	24.5166	9.54312	9.54312	9.54255
10	24.6507	24.6507	24.6531	9.3481	9.3481	9.34465
20	24.6447	24.6447	24.6437	9.21113	9.21113	9.20357

Table 6. Shear buckling coefficients

(a) 0° laminate

	SSSS		CCCC		SSCC		CCSS	
Nv	N_{xy}	N^{u}_{xy}	N_{xy}	N^{u}_{xy}	N_{xy}	N^{u}_{xy}	N_{xy}	N^{u}_{xy}
0.5	10.311	10.311	17.322	17.322	10.9909	10.9909	17.6881	17.6881
1	11.3922	11.3922	19.8345	19.8345	12.5302	12.5302	19.6373	19.6373
5	13.0305	13.0305	23.2361	23.2361	14.85	14.85	22.2833	22.2833
10	13.3242	13.3242	23.6576	23.6576	15.242	15.242	22.645	22.645
20	13.4834	13.4834	23.8465	23.8465	15.4485	15.4485	22.7999	22.7999

(b) Cross-ply laminate ($C_p = 2$)

	SSSS		CCCC		SSCC		CCSS	
Nv	N_{xy}	N^{u}_{xy}	N_{xy}	N^{u}_{xy}	N_{xy}	N^{u}_{xy}	N_{xy}	N^{u}_{xy}
0.5	11.564	11.564	19.1058	19.1058	12.1568	12.1568	18.7211	18.7211
1	12.8196	12.8196	21.7935	21.7935	13.683	13.683	20.8399	20.8399
5	14.5896	14.5896	25.1035	25.1035	15.7773	15.7773	23.4709	23.4709
10	14.8574	14.8574	25.4435	25.4435	16.0966	16.0966	23.7475	23.7475
20	14.9869	14.9869	25.5736	25.5736	16.2585	16.2585	23.8341	23.8341

(c) Cross-ply laminate ($C_P = 1$)

	SSSS		CCCC		SSCC		CCSS	
Nv	N_{xy}	N^{u}_{xy}	N_{xy}	N^{u}_{xy}	N_{xy}	N^{u}_{xy}	N_{xy}	N^{u}_{xy}
0.5	12.5803	12.5803	22.0777	22.0777	14.4076	14.4076	20.4655	20.4655
1	13.881	13.881	25.5331	25.5331	15.871	15.871	22.8321	22.8321
5	15.4648	15.4648	28.7833	28.7833	17.4856	17.4856	25.6343	25.6343
10	15.6275	15.6275	28.9679	28.9679	17.6332	17.6332	25.8538	25.8538
20	15.683	15.683	28.9767	28.9767	17.6813	17.6813	25.8717	25.8717

Table 7. Percentage increase in N_{xy} ($N_v = 5$)

Laminate	SSSS	CCCC	SSCC	CCSS
0 Laminate	14.38	17.15	18.51	13.47
Cross-ply ($C_P = 2$)	13.81	15.19	15.3	12.62
Cross-ply ($C_P = 1$)	11.4	12.73	10.17	12.27

Table 8. Comparison with results obtained by Leissa and Martin (1990)

	Present		Leissa *et al.* (1990)
Composite	N_x	N^{u}_{x}	N_x
Glass–epoxy	13.6923	13.7129	13.0305
Graphite–epoxy	9.6371	9.7323	9.4454
Boron–epoxy	9.0870	9.1803	8.9420

in the literature. The paper explores the concept of designing improved, inhomogeneous plate elements that capitalize upon the new degrees of freedom offered by fibrous composites. A general approach is presented for uniaxial and shear buckling analysis of rectangular, inhomogeneous, orthotropic, laminated composite plates under a variety of combinations of simple and clamped edges. The classical analogy between plate bending and stretching is used to present a unified treatment of the subject matter. A Ritz method, employing Gram–Schmidt orthogonal polynomial sequences, is the basis of the analysis and computation.

In principle, the true stress distribution must be used in the buckling analysis to ascertain its accuracy. However, once a parametric study has been carried out on the basis of the formal two-dimensional elasticity solution, it is possible to identify the regime of behavior where the assumption of uniform prebuckling could offer considerable simplification without admitting much error. The important findings in the case of uniaxial compression are, the stress concentration for a sinusoidal distribution of fibers is not severe (maximum about 10%), the prebuckling stress field has little influence on the buckling load and cross-ply construction in uniaxial compression is more efficient when the loaded edges are simply supported. Uniaxial and shear buckling loads, as a rule, increase by keeping a higher fiber concentration at the centre over the edges.

The paper suggests a more practical way of designing inhomogeneous laminates that significantly improves the axial and shear buckling resistance. Although, the sinusoidal fiber distribution studied herein may not be truly optimal in a strict and formal sense, it provides motivation for a sophisticated optimization study. At present, the technological feasibility of such designs is questionable, nevertheless, the future possibilities arising from a synergism of composite technology with microstructural design are highlighted which must be followed by extensive design–trade studies and experimental verification in order to inspire the necessary confidence in commercial applications.

Acknowledgements—The writers are grateful for support of this work to NSERC of Canada through grant No. A-1582, to the second author (ANS) and to the Province of Ontario through a fellowship (OGS) to the primary author.

REFERENCES

Banichuk, N. V. (1979). Optimization of anisotropic properties of deformable media in plane problems of elasticity. *Mech. Solids* **14**(1), 63–68.
Banichuk, N. V. and Kobelev, V. V. (1981). Optimization of structures made of randomly reinforced composites. *Mech. Compos. Mater.* **4**, 668–676.
Bassily, S. F. and Dickinson, S. M. (1977). The plane stress problem for rectangular regions treated using functions related to beam flexure. *Int. J. Mech. Sci.* **19**, 639–650.
Bendsoe, M. P. and Kikuchi, N. (1988). Generating optimal topologies in structural design using a homogenization method. *Comput. Meth. Appl. Mech. Engng* **71**(2), 197–224.
Bhat, R. B. (1985). Natural frequencies of rectangular plates using characteristic orthogonal polynomials in Rayleigh–Ritz method. *J. Sound Vibr.* **102**, 493–499.
Capey, E. C. (1956). The buckling under longitudinal compression of a simply supported panel that changes in thickness across the width. R.A.E. Tech. Note 174.
Elias, Z. M. (1966). On the duality between the problem of stretching and of bending of plates. NASA CR-705.
Haichang, Hu (1984). Variational principles of theory of elasticity with applications. Gordon and Breach, New York.
Hirano, Y. (1979). Optimum design of laminated plates under axial compression. *AIAA Jl* **17**, 1017–1019.
Jones, R. M. (1975). *Mechanics of Composite Materials*. McGraw-Hill, New York.
Kartvelishivli, V. M. and Kobelev, V. V. (1984). Rational schemes for reinforcing laminar plates from composite materials. *PMM* **48**, 40–49.
Leissa, A. W. and Martin, A. F. (1990). Vibration and buckling of rectangular composite plates with variable fiber spacing. *Int. J. Compos. Struct.* **14**(4), 339–357.
Leissa, A. W. and Vagins, M. (1978). The design of orthotropic materials for stress optimization. *Int. J. Solids Structures* **14**, 517–526.
Mallick, P. K. (1988). *Fiber-Reinforced Composites*. Marcel Dekker, New York.
Mansfield, E. H. (1959). On the buckling of certain optimum plate structures with linearly varying thickness. *Aero. Q.* **10**(2), 145–148.
Martin, A. F. and Leissa, A. W. (1989). Application of the Ritz method to plane elasticity problems for composite sheets with variable fibre spacing. *Int. J. Numer. Meth. Engng* **28**, 1813–1825.
Oda, J. (1988). On optimality of structural and material composition of Bamboo. *Structural Optimization, Proc. IUTAM Symp.* (Edited by G. I. N. Rozvany and B. L. Karihaloo), pp. 201–208.
Pandey, M. D. and Sherbourne, A. N. (1991). Buckling of anisotropic composite plates under stress gradient. *J. Engng Mech., ASCE* **117**(2), 260–275.
Parsons, H. W. (1955). The buckling under compression of a thin rectangular plate of variable thickness. Aero. Res. Council Paper 17231 (Struct. 1759).
Rammerstorfer, F. G. (1974). On the optimal distribution of the Young's modulus of vibrating prestressed beam. *J. Sound Vibr.* **37**, 140–145.
Sherbourne, A. N. and Pandey, M. D. (1991). Optimal fiber distribution for composite plates. *Proc. ASCE Speciality Conf. Advanced Composite for Civil Engng Struct.*, Las Vegas, pp. 81–92.
Southwell, R. V. (1950). On the analogues relating flexure and extension of flat plates. *Q. J. Mech. Appl. Math.* **3**(3), 257–270.
Spillers, W. R. and Levy, R. (1990). Optimal design for plate buckling. *J. Struct. Engng, ASCE* **116**(3), 850–858.
Whitney, J. M. (1987). *Structural Analysis of Laminated Anisotropic Plates*. Technomic Publishing Co., Lancaster, PA.